Supplementary Information

Mechanical folding and unfolding of protein barnase at the single-molecule level

A. Alemany[†,*], B. Rey-Serra[†,*], S. Frutos[†,‡], C. Cecconi[§], F. Ritort[†,‡,**]

[†] Small Biosystems Lab, Departament de Física Fonamental, Universitat de Barcelona, Avda. Diagonal 645, 08028 Barcelona, Spain; [‡] Networking Research Center of Bioengineering, Biomaterials and Nanomedicine (CIBER-BBN), Instituto Carlos III, C/ Sinesio Delgado 4, 28029 Madrid, Spain; § Department of Physics, Informatics and Mathematics, University of Modena and Reggio Emilia, Via Guiseppe Campi, 41125 Modena, Italy; CNR Institute of Nanosciences S3, Via Giuseppe Campi, 41125 Modena, Italy;

[*] Equally contributed. [**] Corresponding author.

Contents

S1 Preparation of barnase

Protein Expression: In-vivo Barnase appears always together with its inhibitor Barstar; if not, barnase becomes lethal to cells. In order to express Barnase we introduced a single site mutation H102A in the gene expressing plasmid which is known to inactivate the enzymatic hydrolyzing activity of Barnase through replacement of a side chain directly involved in substrate binding or catalysis. This mutant is inactive but it is still folded: such mutation has been shown to suppress toxicity of barnase which nonetheless shows activity at non-enzymatic levels, suggesting that the structural disturbances in the folded state are mainly restricted to the side chain [1, 2].

The aminoacid sequence of protein barnase was cloned into the pET100/D-TOPO vector from Invitrogen. This vector contain a His-taq the N-terminus. After cloning of barnase sequence into the pET vector we introduced two cysteines to pull the protein from its ends. These residues were introduced using quick-change mutagenesis. E. coli BL21(DE3) cells (Novagen, Darmstadt, Germany) were transformed with the plasmid and grown at 37℃ in LB (Luria Bertani). Upon reaching an OD_{600} ∼0.8, protein expression was induced with 0.5 mM IPTG (Isopropyl β-D-1-thiogalactopyranoside) at 37℃ for 5 h. The cells were centrifuged and the pellet suspended in five volumes of lysis buffer (50 mM Tris-HCl pH 7.9, 2 mM EDTA, 100 mM NaCl). Cells were lysed by passage through a French press and the soluble proteins isolated by centrifugation at 16000 rpm for 30 minutes. The resulting supernatant was loaded onto a Co-TALON affinity column. The resin was washed with TALON equilibration buffer and the fusion protein eluted from the column in 2 mL fractions with TALON elution buffer. The fractions were analyzed by SDS-PAGE and those containing the fusion protein were pooled. Then the sample was concentrated and purified by size exclusion chromatography using 50 mM $NaHPO_4$, 100 mM NaCl, 1 mM DTT, pH 7.0. The fractions were analyzed by SDS-PAGE and the pure protein was pooled and subsequently 3 mM DTT was added.

DTDP activation of cysteine-modified proteins: The resulting protein was reacted with a concentrated stock of DTDP (10 mM in 0.1 M NaH_2PO_4/Na_2HPO_4, pH 5.5, 15% acetonitrile) such that DTDP was in a 25-fold molar excess of the protein, and allowed to react for 24 h at RT. The excess of DTDP was then removed by dialysis at 4℃. The protein is then activated and ready to be attached to DNA handles. The activated protein was stored at 4℃. ESI-MS was used to confirm the activation of the protein.

Generation of DNA handles: The 500 bp DNA handles were generated in large quantities by PCR using Taq DNA polymerase and the pBR322 plasmid as template. Usually

400 μg of handles were generated at a time using 7 mL of PCR reaction. The two types of handles were generated using the primer 5' Thiol-CAGTTC TCCGCAAGAATTG together with either the primer 5' Bio-GGAATCTTGCACGCCCTCGC or the primer 5 digoxigenin-GGAATCTTGCACGCCCTCGC. The PCR products were purified using HiSpeed Plasmid Maxi Kit, from QIAGEN adding 3 mM DTT in the final elution buffer.

DNA–Protein Coupling: The two types of handles are mixed in equal amounts to obtain digoxigenin/biotin (dig/bio) handles. Then, the handles mixture was reduced with 30 mM DTT at RT for 1 h and concentrated down to 50–60 mL with a 30-kDa MWCO Microcon centrifuge tube. Reducing agents are removed from the handles by sequentially spinning them through three Micro Bio-Spin P6 columns equilibrated with the spin column buffer. The resulting DNA molecules were immediately reacted with a thiol-pyridine activated protein solution (protein molar ratio of 4:1; typically, $\sim$ 20 mM of DNA handles are reacted with $\sim$ 5 mM of activated protein). The reaction is allowed to proceed O/N at RT. The extent of the DNA–protein coupling was assessed by a 4% SDS–PAGE gel.

S2 Elastic models

The elastic response of the peptide chain is assumed to satisfy the ideal WLC model [3], given by:

$$k_{\mathrm{c}}(x) = \frac{k_{\mathrm{B}}T}{PL}\left[\frac{1}{2\left(1-x/L\right)^{3}} + 1 + \sum_{n=2}^{7} n a_n \left(\frac{x}{L}\right)^{n-1}\right], \tag{S1}$$

where x is the equilibrium end-to-end distance of the peptide chain, P is the persistence length and $L = n_{\mathrm{aa}} d_{\mathrm{aa}}$ is the contour length of the peptide. n_{aa} is the total number of aminoacids, equal to 110 for barnase, while d_{aa} is the equilibrium distance between consecutive aminoacids. Numerical coefficients a_n ($n = 2, \ldots, 7$) depend on the analytical expression used to model the WLC behavior. According to truncated version presented in reference [4], these are equal to zero, whereas in reference [5] a numerical expansion of the model is presented which leads to the following values: $a_2 = -0.5164228$, $a_3 = -2.737418$, $a_4 = 16.07497$, $a_5 = -38.87607$, $a_6 = 39.49944$, and $a_7 = -14.17718$.

The globular structure is modeled as a single bond of length $d = 3$ nm (end-to-end distance of the protein at zero force as has been measured by ^{1}H-Nuclear magnetic resonance chemical shifts [6]) that is oriented under mechanical force as a single magnetic dipole does under applied magnetic field [3]. Consequently k_{d} satisfies:

$$k_{\mathrm{d}}^{-1}(f) = \frac{d^2}{k_{\mathrm{B}}T}\left[-\frac{1}{\sinh^2\left(\frac{fd}{k_{\mathrm{B}}T}\right)} + \left(\frac{k_{\mathrm{B}}T}{fd}\right)^2\right]. \tag{S2}$$

S3 Unfolding kinetic rates from unfolding forces

The unfolding kinetic rate is extracted from the master equation of the survival probability of state F, $P_F(f)$ along the stretching experiment:

$$k_{F\to U}(f) = -r\frac{1}{P_F(f)}\frac{dP_F}{df}. \tag{S3}$$

$P_F(f)$ is extracted from unfolding forces f_U according to:

$$P_F(f) = \frac{n(f_U > f)}{n_t}, \tag{S4}$$

where n_t is the total number of unfolding events and $n(f_U > f)$ is the number of events with an unfolding force larger than f.

S4 Bell-Evans (BE) and Dudko-Hummer-Szabo (DHS) models

The force-dependent survival probabilities of the folded $P_F(f)$ and the unfolded $P_U(f)$ state along the stretching or releasing process satisfy $\frac{dP_F(f)}{df} = -\frac{k_{N\to U}(f)}{r}P_F(f)$ and $\frac{dP_U(f)}{df} = -\frac{k_{N\leftarrow U}(f)}{r}P_U(f)$, respectively, where r is the loading rate in units of pN/s. These differential equations can be solved for some analytical expressions of $k_{F\to U}(f)$ and $k_{F\leftarrow U}(f)$ in order to find analytical expressions for $\langle f_U\rangle$ and $\langle f_F\rangle$ [7, 8, 9, 10, 11, 12, 13].

The BE model introduces the effect of force in the Arrhenius kinetic rate as follows:

$$k_{\to}(f) = k_m \exp\left(\frac{fx^{\ddagger}}{k_{\mathrm{B}}T}\right), \qquad k_m = k_0 \exp\left(-\frac{\Delta G^{\ddagger}}{k_{\mathrm{B}}T}\right), \tag{S5}$$

where $x^{\ddagger}$ is the position of the transition state, $\Delta G^{\ddagger}$ is the height of the kinetic barrier, and k_m is the kinetic rate at zero force. Therefore, when the unfolding kinetic rate $k_{F\to U}(f)$ is assumed to satisfy Eq. (S5) then $x^{\ddagger} = x_U^{\ddagger}$, $\Delta G^{\ddagger} = \Delta G_U^{\ddagger}$ and $k_m = k_m^u$. In contrast, when we are modeling the unfolding kinetic rate $k_{F\leftarrow U}(f)$ then $x^{\ddagger} = -x_F^{\ddagger}$, $\Delta G^{\ddagger} = \Delta G_F^{\ddagger}$ and $k_m = k_m^f$. From Eq. (S5) it can then be shown that:

$$\langle f\rangle = \frac{k_{\mathrm{B}}T}{x^{\ddagger}} \log\left(\frac{x^{\ddagger}r}{k_m k_{\mathrm{B}}T}\right). \tag{S6}$$

The DHS model derives the following analytical expression for the kinetic rate by solving the Kramers equation:

$$k(f) = k_m \left(1 - \gamma\frac{fx^{\ddagger}}{\Delta G^{\ddagger}}\right)^{1/\gamma-1} \exp\left\{\frac{\Delta G^{\ddagger}}{k_{\mathrm{B}}T}\left[1 - \left(1 - \gamma\frac{fx^{\ddagger}}{\Delta G^{\ddagger}}\right)^{1/\gamma}\right]\right\}, \tag{S7}$$

where $\gamma = 1/2$ ($\gamma = 2/3$) for parabolic (linear-cubic) free-energy landscapes. The differential equation for the pulling protocol can be solved, and hence:

$$\langle f\rangle = \frac{\Delta G^{\ddagger}}{\gamma x^{\ddagger}}\left\{1 - \left[\frac{k_{\mathrm{B}}T}{\Delta G^{\ddagger}} \log\left(\frac{k_m k_{\mathrm{B}}T e^{\frac{\Delta G^{\ddagger}}{k_{\mathrm{B}}T}+0.577}}{x^{\ddagger}r}\right)\right]^{\gamma}\right\}. \tag{S8}$$

S5 Folding kinetic rates from passive experiments

In passive experiments the survival probability of the unfolded state, $P_U(t)$, satisfies:

$$P_U(t) = \exp\left[-k_{F\leftarrow U}(f)t\right], \tag{S9}$$

where we assume a two-state folding behavior and $P_U(t=0)=1$. The survival probability $P_U(t)$ can be extracted from the passive experiments carried out at a given preset force f_p according to:

$$P_U(t) = 1 - \frac{n(t_{\rm fold} < t)}{n_t} \tag{S10}$$

where n_t is the total number of trajectories at f_p and $n(t_{\rm fold} < t)$ is the number of events at which barnase folds at times $t_{\rm fold}$ smaller than t. We get $k_{F\leftarrow U}(f)$ by fitting the experimentally measured survival probabilities $P_U(t)$ to Eq. (S9) (Fig. S1).

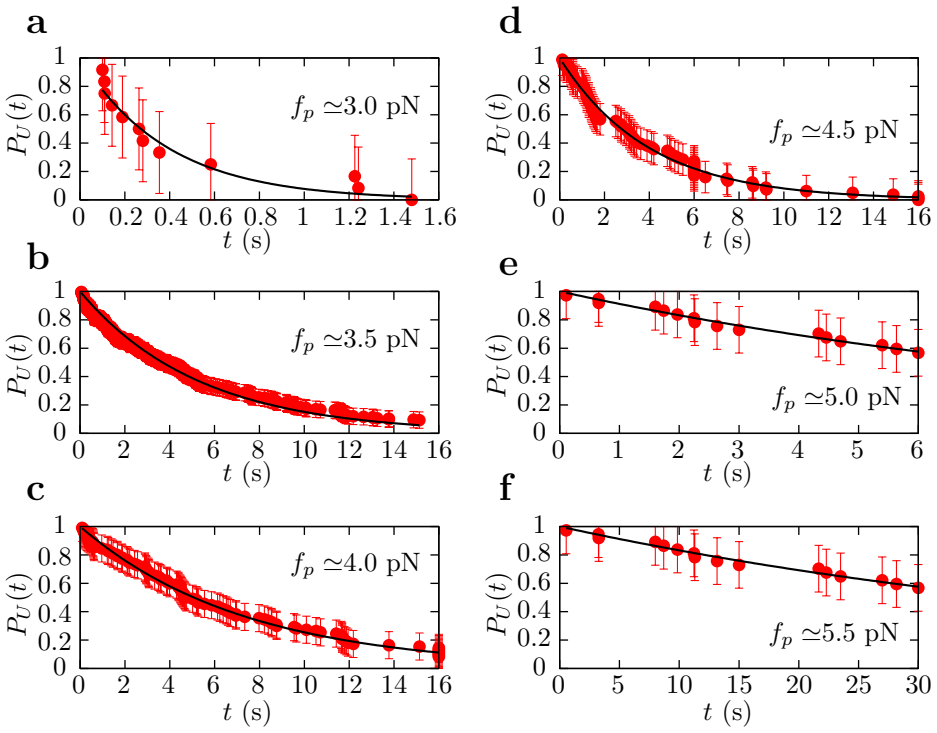

Figure S1: Survival probabailities for state U in passive experiments at different preset forces f_p. Fit of the experimental survival probabilities exracted from passive traces at 3.0 pN (**a**), 3.5 pN (**b**), 4.5 pN (**c**), 5.0 pN (**d**) and 5.5 pN (**e**).

S6 Power spectrum and elastic fluctuations

The power spectrum $S(\nu)$ is defined as the Fourier transform of the force correlation funtion. In Fig. S2 we show results obtained working with a molecular construct that contains no barnase (*i.e.* it is made of handles exclusively) and a full construct made of one barnase and handles, respectively, measured at different values of the force.

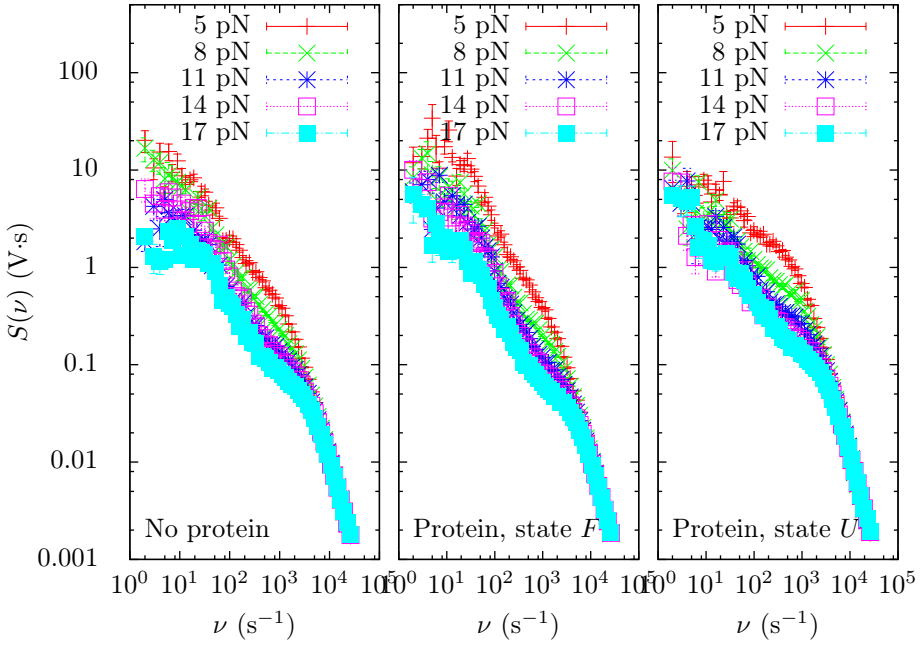

Figure S2: Power spectrums at different forces. Power spectrum of a molecular construction made by the DNA handles without protein (*left*); made by the protein barnase barnase in the folded (F) state and the handles (*center*); and made by the protein barnase in the unfolded (U) state amd the DNA handles (*right*). Data was taken at different preset forces f_p ranging from 2 pN to 23 pN.

In all cases, the resulting power spectrum can be fitted to the double Lorentzian function [14, 15]:

$$S(\nu) = \frac{A_f}{\nu^2 + \nu_f^2} + \frac{A_s}{\nu^2 + \nu_s^2}, \tag{S11}$$

where A_f and ν_f are the amplitude and frequency of the fast mode, and A_s and ν_s of the slow mode. In Fig. S3 we show the results obtained by fitting the power spectrum measured in the presence of protein barnase in the unfolded (U) and the folded (F) state (center and right panels in Fig. S2, respectively). The force-dependence of ν_s suggests that this term is attributed to axial fluctuations occurring in the direction of propagation of the light in the OT. In contrast, ν_f is due to the elastic fluctuations of the molecular

construct tethered between the polystyrene beads. The force-dependent behavior of ν_f does not reveal any signature of the presence of an intermediate state from neither state U or state F. The force-dependent behavior of the amplitudes A_f and A_s does not reveal kinetic effects due to the presence of a possible intermediate, in contrast to the fast protein villin as reported in reference [16]. Hence, no conformational transitions are distinguished in the power spectrum profiles obtained when the protein barnase is either folded or unfolded.

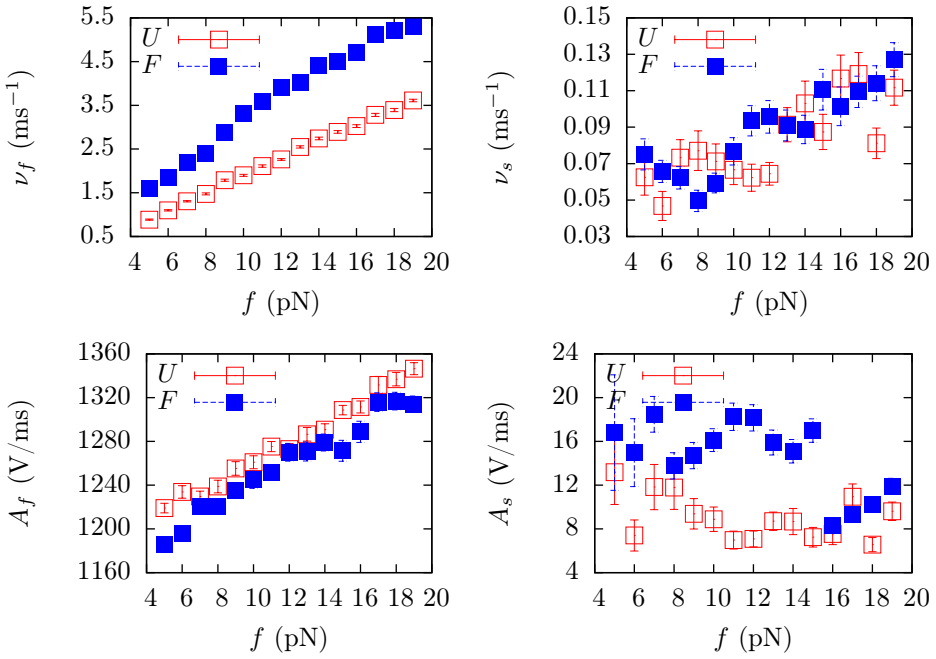

Figure S3: Fit of the power spectrum to a double Lorentzian expression. Power spectra measured at different forces for the two conformational states of protein barnase (folded and unfolded; Fig. S2 center and right panels, respectively) are fitted to a double Lorentzian function (Eq. S11). The resulting force-dependent behavior of the frequencies and the amplitudes is shown.

By modeling the Brownian motion of the bead in the optical trap with the Langevin equation it is shown that the fast frequency mode (*i.e.* the elastic fluctuations) satisfy $\nu_f^F = k_{\text{eff}}^F/\eta$ and $\nu_f^U = k_{\text{eff}}^U/\eta$, being $\eta = 2.6 \times 10^{-4}$ pN·s/nm the water friction coefficient at 25°C for a micro-sphere ($\eta = 6\pi\alpha R$, where $\alpha = 9.1 \times 10^{-3}$ Pa·s is the water viscous coefficient and $R = 1.5$ μm is the radius of the bead captured in the optical trap).

Therefore, according to Eqs. (1) and (2) (main text):

$$\frac{1}{\nu_f^U} - \frac{1}{\nu_f^F} = \eta \left(\frac{1}{k_{\text{eff}}^U} - \frac{1}{k_{\text{eff}}^U} \right) \tag{S12}$$

$$= \eta \left(\frac{1}{k_{\text{p}}(f)} - \frac{1}{k_{\text{d}}(f)} \right). \tag{S13}$$

Hence, according to Eq. (S12) it is possible to extract the elastic properties of the peptide chain by fitting the subtraction of the inverse of the fast frequency modes obtained when barnase is either unfolded or folded (lhs of Eq. S12) to the subtraction of the inverse of the stiffness of the peptide chain and the inverse of the stiffness of barnase when it is in the folded state (rhs of Eq. S13). Results are shown in Fig. S4 for the two analytical expressions for the WLC elastic model used in this work (Eq. S1). Results are compatible with the ones determined by measuring the effective stiffness of the system as described in Section S1.

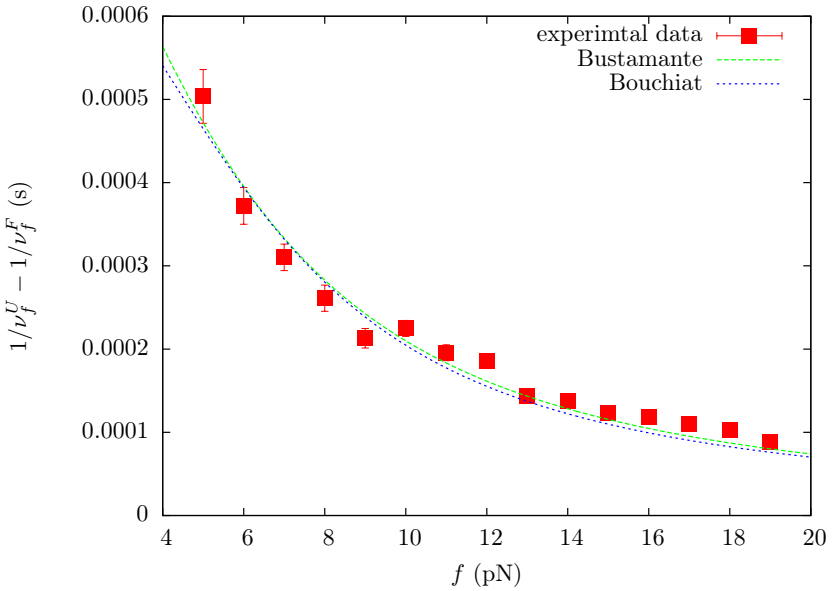

WLC model (ref.)	P (nm)	d_{aa} (nm/aa)
[4]	0.76±0.05	0.35±0.01
[5]	0.59±0.05	0.33±0.01

Figure S4: Elastic response of the peptide chain. Experimental measurement of $\frac{1}{\nu_f^U} - \frac{1}{\nu_f^F}$ and fit to Eq. S12 using the WLC elastic model (Eqs. S1 and S2). The resulting values for P and d_{aa} are given in the Table. Error bars are standard statistical errors.

S7 Continuous Effective Barrier Analysis (CEBA)

According to the Arrhenius phenomenological law, the kinetic rates $k_{F\to U}(f)$ and $k_{F\leftarrow U}(f)$ can be written in terms of the exponential of the kinetic barrier $B(f)$, which corresponds to the free energy of the TS mediating such a transition [17, 18]. Hence:

$$k_{F\to U}(f) = k_0 \exp\left(-\frac{B(f)}{k_{\mathrm{B}}T}\right) \tag{S14a}$$

$$k_{F\leftarrow U}(f) = k_0 \exp\left(-\frac{B(f) - \Delta G(f)}{k_{\mathrm{B}}T}\right). \tag{S14b}$$

k_0 is the attempt frequency at zero force and $\Delta G(f)$, the free energy difference between the unfolded and the folded state at force f, equals:

$$\Delta G(f) = \Delta G_0 - \int_0^f x_{\mathrm{c}}(f)df + \int_0^f x_{\mathrm{d}}df, \tag{S15}$$

where ΔG_0 is the free energy at zero force, $x_{\mathrm{c}}(f)$ is the end-to-end distance of the peptide chain in state U that satisfies the WLC model (Eq. S1) and $x_{\mathrm{d}}(f)$ is the projection along the force axis of the protein diameter (Eq. S2). By inverting Eq. (S14) we get:

$$B(f) = k_{\mathrm{B}}T\left[\log k_0 - \log k_{F\to U}(f)\right] \tag{S16a}$$

$$B(f) = k_{\mathrm{B}}T\left[\log k_0 - \log k_{F\leftarrow U}(f)\right] + \Delta G(f) \tag{S16b}$$

$$= k_{\mathrm{B}}T\left[\log k_0 - \log k_{F\leftarrow U}(f)\right] + \Delta G_0 - \int_0^f x_{\mathrm{c}}(f)df + \int_0^f x_{\mathrm{d}}df. \tag{S16c}$$

Hence, the force-dependent profile of the kinetic barrier between states F and U, $B(f)$, can be determined from the logarithm of experimentally measured unfolding and folding kinetic rates and the theoretical evaluation of the integrals in Eq. (S16c) using the WLC model. In addition, the CEBA methods provides estimations of the attempt frequency at zero force and the free energy of the molecule at zero force from the force-dependent kinetic rates. The steps to follow are as follows:

1. Extract the logarithm (with a minus sign) of the experimentally measured $k_{F\to U}(f)$ and $k_{F\leftarrow U}(f)$ (Eq. S16).

2. Compute the following integrals:

$$I_1 = \int_0^f x_{\mathrm{c}}(f)df \qquad\qquad I_2 = \int_0^f x_{\mathrm{d}}df, \tag{S17}$$

for all force values f at which $k_{F\leftarrow U}(f)$ has been measured. Then, according to Eq. (S16c) compute $-\log k_{F\leftarrow U}(f) - I_1 + I_2$ for each measurement.

3. Shift vertically the quantity $-\log k_{F\leftarrow U}(f) - I_1 + I_2$ in order to match the force-dependent behavior obtained for $-\log k_{F\rightarrow U}(f)$. The amount of the shift equals the free energy of formation ΔG_0 of the molecule.
   The CEBA method has been successfully applied to until now to nucleic acid hairpins, whose force-dependent kinetic rates $k_{F\rightarrow U}(f)$ and $k_{F\leftarrow U}(f)$ were measured at a similar range of forces and hence the matching could be performed straightforwardly [17, 18]. The case of protein barnase is starkly different, since a gap of ~ 7 pN is found between the maximum force value at which $k_{F\leftarrow U}(f)$ is measured and the minimum force value at which $k_{F\rightarrow U}(f)$ is measured (Fig. 3c). In order to perform the matching, we merge together the experimentally measured data points for $-\log k_{F\rightarrow U}(f)$ and $-\log k_{F\leftarrow U}(f) - I_1 + I_2 + \Delta G_0^*$ for different values of ΔG_0^*, and perform a quadratic fit on the resulting data set. The value of ΔG_0^* with the best quadratic fit (or, equivalently, at which χ^2 is minimum) corresponds to ΔG_0. The dashed-gray line in Fig. 5a corresponds to the best fit, where $\Delta G_0 = 20 \pm 5\ k_{\mathrm{B}}T$. Fig. S5 shows the value of χ^2 for different values of ΔG_0^*.

4. The previous fit gives $B(f) - k_{\mathrm{B}}T \log k_0$. By assuming that at large forces ($f < 25$ pN) the kinetic barrier $B(f)$ vanishes, we can get a lower estimation for $\log k_0$ (Fig. 5a).

Finally, it can be shown that:

$$x_U^{\ddagger}(f) = -\frac{\partial B(f)}{\partial f}. \tag{S18}$$

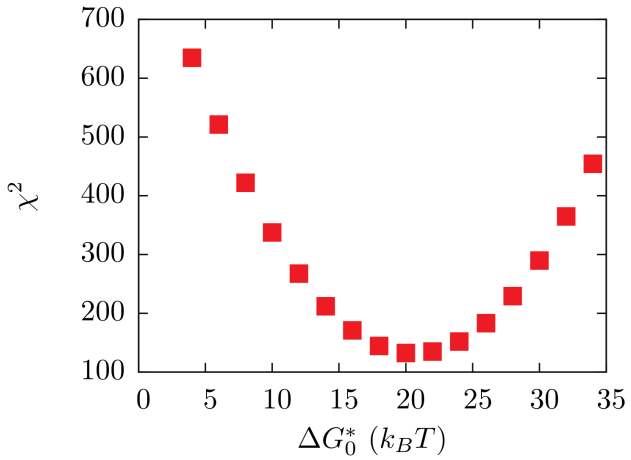

Figure S5: χ^2 test and CEBA method.

S8 Fluctuation relations in presence of Bias

The Jarzynski free energy estimator for a collection of independent irreversible work measurements between well-defined initial and final states reads as [19]:

$$\Delta G = -\log\left[\frac{1}{n}\sum_{i=1}^{n}\exp\left(-\frac{W_i}{k_{\mathrm{B}}T}\right)\right], \tag{S19}$$

where n is the number of work measurements W_i, k_{B} is the Boltzmann constant and T the absolute temperature (taken equal to 298 K). Equation (S19) is highly biased when hysteresis effects are present in the experiments. In order to improve the estimation of the free energy, in ref. [20] the authors provide an analytical expression for the bias given by:

$$B_n = \mu + \log n - \Omega\,(\log n)^{1/\delta} - \lambda^{(1-\delta)/\delta}\left[\gamma_{\mathrm{E}} + \frac{1-\delta}{\delta}\log\Big(\log n\Big) + \log\frac{q}{\delta}\right], \tag{S20}$$

where $\gamma_{\mathrm{E}} = 0.577215665$ is the Euler-Mascheroni constant; Ω and δ are parameters determined by fitting the work distribution's left-most tail to the following expression:

$$P(W) \sim \frac{q}{\Omega}\exp\left(-\frac{|W - W_{\max}|}{\Omega}\right)^{\delta}; \tag{S21}$$

and μ and λ are defined as:

$$\mu = (\delta - 1)\left(\frac{\Omega}{\delta}\right)^{\frac{\delta}{\delta-1}}, \qquad \lambda = \log n\left(\frac{\delta}{\Omega}\right)^{\frac{\delta}{\delta-1}}. \tag{S22}$$

Now, the expression:

$$\Delta G^{*} = -\log\left[\frac{1}{n}\sum_{i=1}^{n}\exp\left(-\frac{W_i}{k_{\mathrm{B}}T}\right)\right] - B_n, \tag{S23}$$

is a proper estimate of the free-energy difference in systems with high dissipation.

In Fig. 5b the fits of the left-most tails of the work distributions obtained in stretching and releasing experiments to Eq. (S21) are shown. In each case, the term $W_{\max}$ is fixed at the value of the work at which the experimental distribution has the maximum, Ω is related to the variance of the distribution, q is a normalization constant, and δ is related to the shape of the tail and must be larger than 1. Results are $W_{\max} = 1121 \pm 3\ k_{\mathrm{B}}T$, $\Omega = 15 \pm 1\ k_{\mathrm{B}}T$, $q = 0.57 \pm 0.05\ k_{\mathrm{B}}T$ and $\delta = 1.90 \pm 0.05\ k_{\mathrm{B}}T$ for

stretching; and $W_{\max} = 1022 \pm 1\ k_{\mathrm{B}}T$, $\Omega = 7 \pm 1\ k_{\mathrm{B}}T$, $q = 0.55 \pm 0.06\ k_{\mathrm{B}}T$ and $\delta = 1.80 \pm 0.05\ k_{\mathrm{B}}T$ for releasing.

S9 Energetic contributions from the experimental setup

The free-energy difference ΔG (or ΔG^*) determined from fluctuation relations contains contributions from the molecule, the handles and the bead in the optical trap, as follows:

$$\Delta G = \Delta G_0 + \Delta W_{\rm st} + \Delta W_{\rm handles} + \Delta W_{\rm bead}. \tag{S24}$$

ΔG_0 is the free energy of formation of the molecule at zero force. $\Delta W_{\rm st} = W_{\rm st}^U - W_{\rm st}^N$ is the difference between the reversible work needed to stretch the unfolded protein from 0 to $f_{\rm max}$ (force applied to the molecular system at λ_1) and the reversible work needed to align the folded protein along the force axis from 0 to $f_{\rm min}$ (force applied to the molecular system at λ_0):

$$\Delta W_{\rm st} = \int_0^{x_U(f_{\rm max})} f_U(x')dx' - \int_0^{x_N(f_{\rm min})} f_N(x')dx', \tag{S25}$$

where $f_U(x)$ ($f_N(x)$) and the inverse function $x_U(f)$ ($x_N(f)$) are the equation of state of the unfolded (folded/native) protein. The first integral is computed using the WLC model (Eq. S1) with persistence length $P = 0.60 \pm 0.05$ nm and inter-aminoacid distance $d_{\rm aa} = 0.34 \pm 0.01$ nm/aa. The second integral is computed according to Eq. (S2). $\Delta W_{\rm handles}$ is the reversible work needed to stretch the handles form $f_{\rm min}$ to $f_{\rm max}$:

$$\Delta W_{\rm handles} = \int_{x_{\rm handles}(f_{\rm min})}^{x_{\rm handles}(f_{\rm max})} f_{\rm handles}(x')dx', \tag{S26}$$

where $f_{\rm handles}(x)$ and the inverse $x_{\rm handles}(f)$ are the state equation of the dsDNA handles, modeled according to the extensible WLC model where the Bouchiat interpolation formula is used [5]. The elastic parameters are taken from ref. [14], where experiments with similar ionic concentrations as the ones used here are performed [14]. Hence, the persistence length is equal to $P = 34 \pm 5$ nm, the Young modulus $S = 850 \pm 100$ pN and the interphosphate distance $d_b = 0.34$ nm/base. $\Delta W_{\rm bead}$ is the reversible work needed to pull the trapped bead from $f_{\rm min}$ to $f_{\rm max}$:

$$\Delta W_{\rm bead} = \int_{x_{\rm bead}(f_{\rm min})}^{x_{\rm bead}(f_{\rm max})} f(x')dx' = \int_{f_{\rm min}}^{f_{\rm max}} \frac{f'}{k_{\rm bead}(f')} df'. \tag{S27a}$$

Here, the force-dependent strap stiffness determined by N. Forns and collaborators for the mini-tweezers is used [21], $k_{\rm bead}(f) = 0.062 + 0.00059 f$ pN/nm.

References

[1] Axe, D. D. , N. W. Foster, and A. R. Fersht. 1998. A search for single substitutions that eliminate enzymatic function in a bacterial ribonuclease. Biochemistry. 37:7157–7166.

[2] Cioffi, M., C. A. Hunter, M. Pandya, M. J. Packer, and M. P. Williamson. 2009. Use of quantitative 1H NMR chemical shift changes for ligand docking into barnase. J. Biomol. NMR. 43:11–19.

[3] Alemany, A., and F. Ritort. 2014. Determination of the elastic properties of short ssDNA molecules by mechanically folding and unfolding DNA hairpins. Biopolymers. 101:1193–1199.

[4] Bustamante, C., J. Marko, E. D. Siggia, and S. B. Smith. 1994. Entropic elasticity of λ-phage DNA. Science. 265:1599–160

[5] Bouchiat, C., M. D. Wang, J. F. Allemand, T. Strick, S. M. Block, and V. Croquette. 1999. Estimating the persistence length of a worm-like chain molecule from force-extension measurements. Biophys. J. 76:409–413.

[6] Wilton, D. J., R. Kitahara, K. Akasaka, M. J. Pandya, and M. P. Williamson. 2009. Pressure-dependent structure changes in barnase on ligand binding reveal intermediate rate fluctuations. Biophysical J. 97:1482–1490.

[7] Bell, G. I. 1978. Models for the specific adhesion of cells to cells. Science. 200:618–627.

[8] Evans, E., and K. Ritchie. 1997. Dynamic strength of molecular adhesion bonds. Biophys. J. 72:1541–1555.

[9] Merkel, R., P. Nassoy, A. Leung, K. Ritchie, and E. Evans. 1999. Energy landscapes of receptor–ligand bonds explored with dynamic force spectroscopy. Nature. 397:50–53.

[10] Evans, E. 2001. Probing the relation between force-lifetime-and chemistry in single molecular bonds. Annu. Rev. Biophys. Biomol. Struct. 30:105–128.

[11] Dudko, O. K., G. Hummer, and A. Szabo. 2006. Intrinsic rates and activation free energies from single-molecule pulling experiments. Phys. Rev. Lett. 96:108101.

[12] Dudko, O. K., J. Mathé, A. Szabo, A. Meller, and G. Hummer. 2007. Extracting kinetics from single-molecule force spectroscopy: nanopore unzipping of DNA hairpins. Biophys. J. 92:4188–4195.

[13] Dudko, O. K., G. Hummer, and A. Szabo. 2008. Theory, analysis, and interpretation of single-molecule force spectroscopy experiments. Proc. Natl. Acad. Sci. U. S. A. 105:15755–15760.

[14] Ribezzi-Crivellari, M., and F. Ritort. 2012. Force Spectroscopy with Dual-Trap Optical Tweezers: Molecular Stiffness Measurements and Coupled Fluctuations Analysis. Biophys. J. 103:1919–1928.

[15] Ribezzi-Crivellari, M., A. Alemany, and F. Ritort. 2015. Universal Axial Fluctuations in Optical Tweezers. Opt. Lett. 40:800–803.

[16] Žoldák, G., J. Stigler, B. Pelz, H. Li, H. and M. Rief. 2013. Ultrafast folding kinetics and cooperativity of villin headpiece in single-molecule force spectroscopy. Proc. Natl. Acad. Sci. U. S. A. 110:18156–61.

[17] Manosas, M., D. Collin, and F. Ritort. 2006. Force-dependent fragility in RNA hairpins. Phys. Rev. Lett. 96:218301.

[18] Bizarro, C. V., A. Alemany, and F. Ritort. 2012. Non-specific binding of Na^{+} and Mg^{2+} to RNA determined by force spectroscopy methods. Nucleic Acids Res. 40:6922–6935.

[19] Jarzynski, C. 1997. Nonequilibrium equality for free energy differences. Phys. Rev. Lett. 78:2690.

[20] Palassini, M., and F. Ritort. 2011. Improving free-energy estimates from unidirectional work measurements: theory and experiment. Phys. Rev. Lett. 107:060601.

[21] Forns, N., S. de Lorenzo, M. Manosas, K. Hayashi, J. M. Huguet, and F. Ritort. 2011. Improving signal/noise resolution in single-molecule experiments using molecular constructs with short handles. Biophys. J. 100:1765–1774.